Acta Neurologica Scandinavica

Acta Neurol Scand 2016: 134: 67–75 DOI: 10.1111/ane.12515

ACTA NEUROLOGICA
SCANDINAVICA

Variants in the genes *DCTN2*, *DNAH10*, *LRIG3*, and *MYO1A* are associated with intermediate Charcot–Marie–Tooth disease in a Norwegian family

Braathen GJ, Høyer H, Busk ØL, Tveten K, Skjelbred CF, Russell MB. Variants in the genes *DCTN2*, *DNAH10*, *LRIG3*, and *MYO1A* are associated with intermediate Charcot–Marie–Tooth disease in a Norwegian family.
Acta Neurol Scand 2016: 134: 67–75.

Introduction – Charcot–Marie–Tooth disease (CMT) is a heterogeneous inherited neuropathy. The number of known CMT genes is rapidly increasing mainly due to next-generation sequencing technology, at present more than 70 CMT-associated genes are known. We investigated whether variants in the *DCTN2* could cause CMT. *Material and methods* – Fifty-nine Norwegian CMT families from the general population with unknown genotype were tested by targeted next-generation sequencing (NGS) for variants in *DCTN2* along with 32 CMT genes and 19 other genes causing other inherited neuropathies or neuronopathies, due to phenotypic overlap. In the family with the *DCTN2* variant, exome sequencing was then carried out on all available eight family members to rule out the presence of more potential variants. *Results* – Targeted NGS identified in one family a variant of *DCTN2*, c.337C>T, segregating with the phenotype in five affected members, while it was not present in the three unaffected members. The *DCTN2* variant c.337C>T; p.(His113Tyr) was neither found in in-house controls nor in SNP databases. Exome sequencing revealed a singular heterozygous shared haplotype containing four genes, *DCTN2*, *DNAH10*, *LRIG3*, and *MYO1A*, with novel sequence variants. The haplotype was shared by all the affected members, while the unaffected members did not have it. *Conclusions* – This is the first time a haplotype on chromosome 12 containing sequence variants in the genes *DCTN2*, *DNAH10*, *LRIG3*, and *MYO1A* has been linked to an inherited neuropathy in humans.

G. J. Braathen[1,2,3], H. Høyer[1,2,3], Ø. L. Busk[3], K. Tveten[3], C. F. Skjelbred[3], M. B. Russell[1,2]

[1]Head and Neck Research Group, Research Centre, Akershus University Hospital, Lørenskog, Oslo, Norway; [2]Institute of Clinical Medicine, Campus Akershus University Hospital, University of Oslo, Nordbyhagen, Oslo, Norway; [3]Section of Medical Genetics, Department of Laboratory Medicine, Telemark Hospital, Skien, Norway

Key words: Charcot–Marie–Tooth disease; inherited neuropathy; *DCTN2*; targeted next-generation sequencing; exome sequencing

G. J. Braathen, Head and Neck Research Group, Research Centre, Akershus University Hospital, Sykehusveien 25, 1478 Lørenskog, Norway
Tel.: +4791502900
Fax: +4767968861
e-mail: g.j.braathen@medisin.uio.no

Accepted for publication September 11, 2015

Introduction

Charcot–Marie–Tooth disease (CMT) is the most common inherited neuropathy with a prevalence ratio of 15–82/100,000 in different European settings (1–4). CMT is genetically heterogeneous (The Mutation Database of Inherited Peripheral Neuropathies (IPNMDB) (http://www.molgen.ua.ac.be/cmtmutations/) and Neuromuscular Disease Center (http://neuromuscular.wustl.edu/)). At present, variants in more than 70 different genes can cause CMT, and the number is rapidly increasing mainly due to next-generation sequencing technology (5, 6).

The overexpression of *DCTN2* in transgenic mice disrupts the dynein (DYNC1H1)–dynactin (DCTN1) complex and results in a late-onset slowly

Correction added on 29 October 2015 after first online publication: The 3rd affiliation was previously omitted for authors G.J Braathen and H. Høyer, and this is now corrected in the current version.

progressive motor neuron degenerative disease (7). Although not yet implicated in CMT, it was hypothesized that the gene *DCTN2* might cause CMT.

Despite the high number of currently known CMT genes, there are indications that many genes are yet to be identified; for example, in a Norwegian study investigating 51 neuropathy genes, only 46% of the families received a molecular diagnosis (1, 8).

We tested 59 Norwegian CMT families without identified gene mutations for the presence of *DCTN2* mutations. Then, we did exome sequencing of the identified *DCTN2* family looking for other shared sequence variants that may explain the phenotype.

Material and methods

Study population

We analyzed 59 Norwegian CMT families from eastern Akershus County, irrespective of their neurophysiological phenotype with targeted next-generation sequencing (NGS). These families had previously tested negative for *PMP22* duplication by real-time quantitative PCR followed by sequential point mutation analysis of the genes *PMP22, GJB1*, *MPZ*, *LITAF*, *MFN2*, and *EGR2* by conventional Sanger sequencing (1). Detailed description of the study population, clinical interview, genetic and neurologic examination, neurophysiology, and genetic laboratory tests has been published elsewhere (1, 8). In this study, the 59 families (22 CMT1 families, 29 CMT2 families, one intermediate CMT family, and seven families with unknown neurophysiological phenotype) were investigated for mutations in *DCTN2*. A control group of 180 healthy individuals were included to help differentiate between normal and pathogenic variation (9).

Neuropathy impairment score

Cranial nerves, muscle weakness, reflexes, and sensation were scored according to the Neuropathy Impairment Score (NIS) (10). Muscle strength is scored linearly from 0 to 4; normal strength is scored 0; paralysis is scored 4; and 25% muscle weakness, 50% muscle weakness, and 75% muscle weakness are scored 1, 2, and 3. Movement against gravity, movement with gravity eliminated, and muscle flicker without movement are scored 3.25, 3.5, and 3.75, respectively.

Targeted capture and DNA sequencing

Mutations in *DCTN2* were investigated by adding *DCTN2* to a gene panel for NGS sequencing along with 51 other known inherited neuropathy or neuronopathy genes. The results from the known neuropathy genes have been published elsewhere, such as gene names, GenBank accession and version number, average coverage, % bases $\geq 2\times$ coverage, and % bases $\geq 30\times$ coverage (11). Exome sequencing was performed in the eight family members from the DCTN2 family according to methods published elsewhere (12).

Sequence analysis

Bioinformatic analysis consisted of a standard protocol including image analysis and base calling by Illumina RTA 1.12.4.2, demultiplexing by CASAVA 1.8 (Illumina Inc, San Diego, CA, USA), and alignment of sequence reads to the reference genome GRCh37/hg19 by BWA (13). Picard was used for removing PCR duplicates (http://picard.sourceforge.net/). The genome analysis toolkit (GATK) was applied for base quality score recalibration, insertion and deletion (INDEL) realignment, and single-nucleotide polymorphism (SNP) and INDEL discovery (14, 15). Annotation of sequence variants was performed by Annovar (16). Variants present in exons $\pm$ 10-bp intron sequences, 3′untranslated regions (UTR), and 5′UTR were included in further analysis. Variants were filtered based on frequency data from dbSNP 135, 1000 genomes, 180 in-house normal controls, pathogenicity predictions through the Alamut interface v2.2-0 (Interactive Biosoftware, Rouen, France), and reports in the Human Genome Mutation Database (HGMD), the Mutation Database of Inherited Peripheral Neuropathies (IPNMDB), and published reports.

Verification by Sanger sequencing

The variants identified in the *DCTN2* family were verified by Sanger sequencing in all available family members to establish genotype–phenotype correlation. Primer design and sequence analysis were performed using CLC Main Workbench (CLC bio, Aarhus, Denmark), and the sequencing was carried out using standard procedures and sequenced on the ABI3130XL (Life Technologies Ltd, Paisley, UK) (1).

The variants identified in this family have been submitted to the ClinVar database (http://www.ncbi.nlm.nih.gov/clinvar/).

Variant interpretation

Several tools were utilized for variant effect prediction. Multiple sequence alignment (MSA) was

visualized using Alamut to see conservation across several species (http://www.interactive-biosoftware.com/). The mutation effect predictors Align GVGD, MutationTaster, PolyPhen, SIFT, and SNAP were utilized (17–21). Nucleotide conservation was assessed using phylop (22, 23). Evaluation of biochemical differences was carried out by Grantham distance (24).

Ethics

The study was approved by the Norwegian regional committees for medical and health research ethics. Participation was based on informed consent.

Results

Clinical features

Fig. 1 shows the pedigree. The mode of inheritance is compatible with dominant inheritance. The parents (I-1 and I-2) were second cousins, while II-7 and II-8 were unrelated. I-1 and I-2 had gait problems of unknown cause. I-1 had gait problems and markedly reduced balance, while I-2 had steppage gait. II-1 and II-9 had intellectual deficiency due to birth complications.

The available family members II-3, II-7, II-9, II-10, III-7, III-8, III-9, and III-10 were neurologically examined. II-3, III-7, and III-10 were unaffected. Table 1 shows clinical characteristics of those affected members, that is, II-7, II-9, II-10, III-8, and III-9. Age at onset was late in 4th and 5th decade. The motor signs and severely reduced balance were present in three affected members (II-7, II-10, and III-8), while one affected member (III-9) had minor signs 2 years after the onset, and one (II-9) had an inconclusive neurological examination due to lack of cooperation. One affected member (II-10) also had multiple sclerosis affecting eye movement, and asymmetrical facial and soft palate weakness. Table 2 shows the neurophysiological investigation. The results are compatible with intermediate CMT.

Genetic analyses

We identified a *DCTN2* variant in one of 59 families. In this family, targeted NGS identified two heterozygous variants *DCTN2*, c.337C>T, and *GARS*, c.95T>C, but only the *DCTN2* variant segregated with the phenotype. DNA was available in five affected (II-7, II-9, II-10, III-8, and III-9) and three unaffected (II-3, III-7, and III-10) family members. The *DCTN2* variant c.337C>T, p.(His113Tyr) replaces histidine with tyrosine.

The *GARS* variant c.95T>C, p.(Leu32Pro) replaces leucine with proline and was carried by one unaffected member (III-7) and four affected members (II-7, II-9, II-10, and III-9). III-7 was unaffected at the age of 50, while III-8 was affected and did not carry the *GARS* variant. Thus, the *GARS* variant did not segregate with the CMT phenotype.

To rule out the presence of more potentially pathogenic variants, exome sequencing was performed and analyzed using both dominant and recessive models. There were no homozygous or compound heterozygous variants shared among all of the affected or some of the affected members. The only shared haplotype among the affected is situated on chromosome 12 containing four genes with sequence variants. It is heterozygous, consistent with a dominant model. The haplotype was shared by all the affected members, while the unaffected members did not have it.

Exome sequencing revealed four novel heterozygous sequence variants in different genes on chromosome 12 that were shared among the affected members, while the unaffected members did not have these sequence variants. The genes and transcripts were NM_006400.3 *DCTN2*: c.337C>T (p.His113Tyr), NM_207437.3 *DNAH10*: c.9510C>G (p.Ile3170Met), NM_153377.3 *LRIG3*:

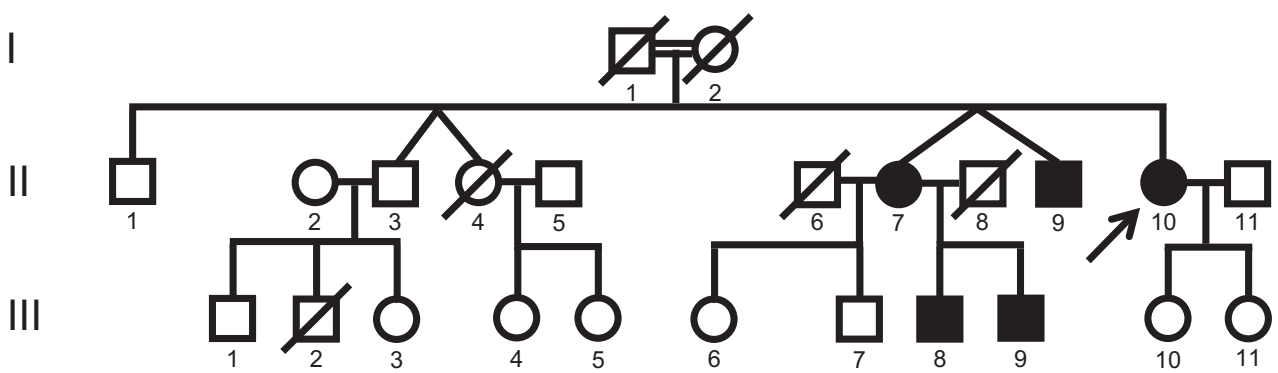

Figure 1. Pedigree of the CMT family with *DCTN2* variant c.337C>T.

Table 1 Clinical characteristics of affected members carrying the *DCTN2*variant

Family members	II-7	II-9	II-10	III-8	III-9
Gender	♀	♂	♀	♂	♂
Age at onset	40	–	35	30	42
Age at investigation	71	63	64	45	44
Clinical characteristics					
Muscle wasting[1]					
Underarm	0	1	0	0	0
Hand	2	2	0	0	0
Thigh	1	1	0	0	0
Leg	1	1	1	0	0
Feet	1	1	1	1	0
Muscle weakness[NIS]					
Facial muscles	0	–	1/0[2]	0	0
Soft palate	0	–	1/0[2]	0	0
Finger spread	2	–	0	0	0
Thumb abduction	2	–	0	0	0
Knee flexion	1	–	0	0	0
Knee extension	1	–	0	0	0
Ankle dorsiflexors	3	–	1	0	0
Ankle plantarflexors	3	–	0	0	0
Toe extensors	3/3.25[2]	–	1	2/3[2]	0
Toe flexors	3	–	1	2	0
Sensory loss					
Touch[1]					
Feet, leg	1	–	1	0	0
Pain[1]					
Overarm	1	–	0	0	0
Hand, underarm	1	–	1	0	1
Thigh	1	–	0	0	0
Feet, leg	2	–	1	1	1
Vibration[1]					
Hand	2	–	1	2	1
2. finger	2		1	0	1
Knee	2	–	2	2	1
Ankle	2	–	2	2	1
1. metatarsal	2	–	2	2	2
1.toe	2	–	2	2	2
Proprioceptive[1]					
Toe	1	–	1	1	0
Reflexes[1]					
Biceps	2	2	1	2	0
Triceps	0	2	1	1	0
Brachioradialis	0	1	0	1	0
Patellar	2	2	2	2	1
Achilles	2	2	2	2	1
Deformities[1]					
Pescavus	2	1	0/1[2]	2	0
Hammertoes	1	–	1	0	0
Pesplanus	0	–	1/0[2]	0	0
Slow eye movement[1]	0	–	1	0	0
Romberg[1]	2	–	2	2	0
NIS	58.25	16[3]	32	37	14

–, not informative; [1]0, normal; 1, mildly/moderately affected modality; 2, severely affected modality. [2]Asymmetrical signs right/left. Neuropathy Impairment Score (NIS): For details, see Methods section. [3]Muscle weakness and sensory signs unknown due to mental retardation.

c.65G>A (p.Gly22Glu), and NM_005379.3 *MYO1A*:c.3128A>T (p.Gln1043Leu). The chromosomal gDNA position for the four heterozygous sequence variants on chromosome 12 ranged from 57422543 to 124393856 with *MYO1A* variant at 57422543, *DCTN2* variant at 57928880, *LRIG3* variant at 59313952, and *DNAH10* variant at 124393856. The affected members did not share homozygous sequence variants nor compound heterozygous variants.

Variant interpretation

The *DCTN2* His113 is a moderately conserved amino acid (Fig. 2), situated in dynamitin subunit 2 and also moderately conserved on the nucleotide level, as shown by a phylop score of 2.95. The *DCTN2* variant, c.337C>T, infers an amino acid change from the basic histidine to a polar uncharged tyrosine, which is a biochemically moderate change with a Grantham distance of 83 (0–215). The variant is predicted neutral by Align GVGD (score: C0 (GV: 160.13 – GD: 0.00)), disease causing by MutationTaster (*P*-value: 0.999), possibly damaging by PolyPhen (score: 0.802), tolerated by SIFT (score: 1), and neutral by SNAP (Table 3). *DNAH10* 3170Ile is a moderately conserved amino acid. The *DNAH10* c.9510C>G infers an amino acid change from the hydrophobic isoleucine to the hydrophobic methionine, which is a biochemically weak change with a Grantham distance of 10. The variant is predicted neutral by Align GVGD (score: C0), disease causing by MutationTaster (*P*-value: 0.998), probably damaging by PolyPhen (score: 0.972), and deleterious by SIFT (score: 0.01).

LRIG3 22Gly is a moderately conserved amino acid. The *LRIG3* c.65G>A infers an amino acid change from the non-polar glycine to a polar glutamic acid, which is a biochemically moderate change with a Grantham distance of 98. The variant is predicted neutral by Align GVGD (score: C0), polymorphism by MutationTaster (*P*-value: 0.969), benign by PolyPhen (score: 0.272), and deleterious by SIFT (score: 0).

MYO1A 1043Gln is a moderately conserved amino acid. The *MYO1A* c.3128A>T infers an amino acid change from the polar glutamine to the hydrophobic leucine, which is a biochemically moderate change with a Grantham distance of 113. The variant is predicted neutral by Align GVGD (score: C0), polymorphism by MutationTaster (*P*-value: 1), benign by PolyPhen (score: 0.012), and tolerated by SIFT (score: 0.19).

Discussion

Methodological considerations

DCTN2 was included in the panel as the overexpression of *DCTN2* in transgenic mice disrupts the dynein (*DYNC1H1*)–dynactin (*DCTN1*)

Table 2 Neurophysiology in affected members carrying the *DCTN2* variant. Abnormal values are in bold

		Age at			Motor nerves								Sensory nerves						
					Median		Ulnar		Peroneal		Tibial		Median		Ulnar		Sural		EMG
	Sex	Onset (yrs)	Examination (yrs)	R/L	CMAP	CV	CMAP	CV	CMAP	CV	CMAP	CV	SNAP	CV	SNAP	CV	SNAP	CV	chronic dener-vation
Normal values→					4.0	49.0	4.0	49.0	3.0	41.0	3.0	41.0	12.0	46.0	17.0	47.0	17.0	44.0	
II-7	♀	40	67	R	**3.6**	**40.0**	4.7	**40.0**	**A**	**A**	**A**	**A**	↓	**29.0**	**0.5**	**29.0**	**A**	**A**	**Present**
				L	–	–	–	–	**A**	**A**	**A**	**A**	–	–	–	–	**A**	**A**	
II-9	♂	–	64	R	**4.2**	**42.0**	**2.9**	**37.3**	**A**	**A**	**A**	**A**	**2.4**	**29.6**	**A**	**A**	**A**	**A**	**Present**
				L	**1.5**	**35.5**	–	–	**A**	**A**	**A**	**A**	–	–	–	–	**A**	**A**	**Present**
II-10	♀	35	46	R	4.0	50.0	–	–	**2.0**	**30.0**	**0.4**	**31.0**	**10.0**	56.0	–	–	**A**	**A**	**Present**
III-8	♂	30	40	R	–	–	–	–	**0.4**	**35.2**	**1.3**	**35.5**	–	–	–	–	**A**	**A**	**Present**
				L	6.8	**45.9**	5.1	**44.9**	**0.7**	**29.8**	**0.7**	**32.2**	**A**	**A**	**A**	**A**	**1.6**	**29.7**	

CMAP, compound motor action potential (mV); SNAP, sensory nerve action potential (μV); CV, conduction velocity (m/s); A, absent evoked response; –, not measured; R/L, right/left.

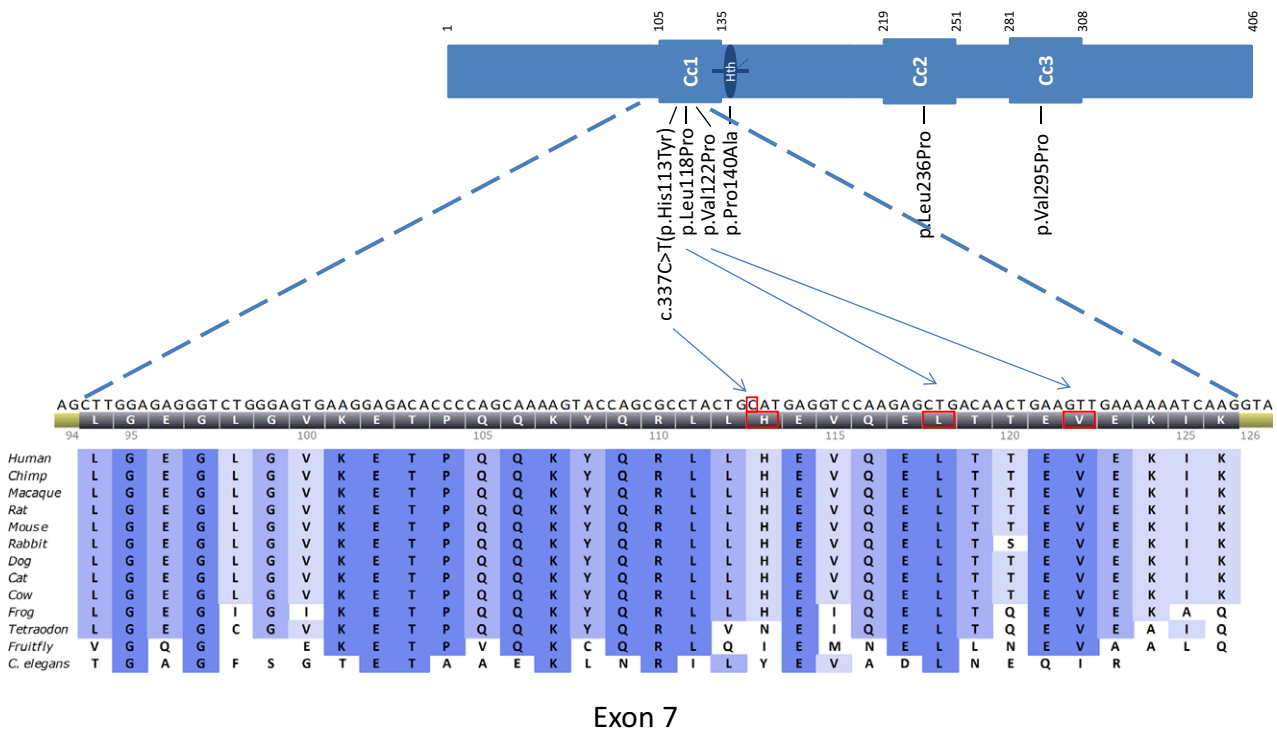

Exon 7

Figure 2. Multiple sequence alignment for *DCTN2*, exon 7, DCTN2 (dynamitin) protein overview with coiled-coil motifs (Cc1, Cc2, Cc3), helix-to-helix motif (Hth), and position of the *in silico* tested variants; it was adapted from references 24 and 30.

complex and results in a late-onset slowly progressive motor neuron degenerative disease (7). Although not yet implicated in CMT, it was hypothesized that the gene *DCTN2* might cause CMT.

Despite the high number of currently known CMT genes, there are indications that many genes are yet to be identified, for example, in a Norwegian study investigating 51 neuropathy genes, only 46% of the families received a molecular diagnosis (1, 8).

A novel heterozygous variant in *DCTN2* c.337C>T was detected in one of the 59 families investigated. The variant was confirmed by Sanger sequencing in all five affected members, while three unaffected members did not have it. The variant was neither seen in the 180 neurologically assessed in-house Norwegian controls nor in the Single Nucleotide Polymorphism Database (dbSNP) 135 (http://www.ncbi.nlm.nih.gov/snp/), Exome Aggregation Consortium (ExAC) (http://exac.broadinstitute.org), GEnomes

Table 3 In silico tests of our variant and dynamitin mutants used in targeted mutagenesis to evaluate how dynamitin's different structural domains contribute to its ability to self-associate, interact with dynactin, and assemble into a complex with its close binding partner, p24

	Motif	Side chain alteration	Phylop score	Grantham distance	Align GVGD (Class)	Mutation Taster	PolyPhen (score)	SIFT (score)	SNAP
Our variant									
His113Tyr	Coiled-coil (Cc1)	Polar→hydrophobic	2.95	**83**	C0 (GV:160.13 – GD:0.00)	**Disease causing**	Possibly damaging (0.802)	Tolerated (1.00)	Neutral
Dynamitin mutants									
Leu11 8Pro (C1)	Coiled-coil (Cc1)	Hydrophobic→ hydrophobic	4.08	**98**	**C65** (GV: 0.00 – GD: 97.78)	**Disease causing**	**Probably damaging** (0.999)	**Deleterious** (0.00)	**Non-neutral**
Val122Pro (C1)	Coiled-coil (Cc1)	Hydrophobic→ hydrophobic	2.55	**68**	C25 (GV: 28.68- GD: 68.57)	**Disease causing***	**Probably damaging** (0.999)	**Deleterious** (0.00)	Neutral
Pro140Ala	Helix-turn-helix	Hydrophobic→ hydrophobic	3.84	27	C0 (GV: 173.88 – GD: 13.77)	**Disease causing**	Possibly damaging (0.802)	Tolerated(0.45)	Neutral
Leu236Pro (C2)	Coiled-coil (Cc2)	Hydrophobic→ hydrophobic	4.40	**98**	**C65** (GV: 4.86 – GD: 95.38)	**Disease causing**	**Probably damaging**(0.994)	**Deleterious**(0.00)	**Non-neutral**
Val295Pro (C3)	Coiled-coil (Cc3)	Hydrophobic→ hydrophobic	4.48	**68**	C0 (GV: 235.27 – GD: 33.99)	**Disease causing***	Possibly damaging(0.574)	**Deleterious** (0.02)	**Non-neutral**

Side chain charges carried at physiological pH 7.4. Phylop score: values between −14 and +6, with positive scores indicating conserved sites. Grantham distance ranges from 0 to 215 (possible scores 5-215). Scores of <50 small biochemical difference, 51 to 151 moderate biochemical difference, and values above 151 have a large biochemical difference. Align GVGD: classes (C0, C15, C25, C35, C45, C55, C65) are computed based on both biochemical difference and multiple sequence alignments. The higher the class, the more likely the change is deleterious. MutationTaster outputs prediction of the effect of the change, along with a probability of 0–1, where a value close to 1 indicates a high probability of the prediction being correct, all with *P*-value ≥0.999. PolyPhen: values >0.5 is likely to affect the protein. SIFT ranges from 0 to 1; scores <0.05 are predicted deleterious, while scores ≥ are tolerated. SNAP outputs an interpretation of the effect of the mutation along with a reliability of this interpretation, all with accuracy >50%. Values affecting protein function in bold.
*Two bases were substituted to achieve this amino acid change.

Management Application (GEM.app) (https://genomics.med.miami.edu/gem-app/), and 1000 genomes (http://www.ncbi.nlm.nih.gov/variation/tools/1000genomes/).

Then, we did exome sequencing of the identified *DCTN2* family looking for other shared sequence variants that may explain the phenotype. Exome sequencing revealed three other heterozygous sequence variants on chromosome 12. Probably, the affected members share an ancestral haplotype containing the four heterozygous sequence variants in the genes *MYO1A, DCTN2*, *LRIG3,* and *DNAH10*. A shared haplotype is compatible with dominant inheritance seen in the pedigree (Fig. 1), and the affected members did not share homozygous sequence variants nor compound heterozygous variants.

Genotype–phenotype correlation

We observed perfect cosegregation of the *DCTN2* variant with the disease in the eight subjects for whom DNA was available A segregation pattern observed in our pedigree could occur by chance in $(½)^7 = 1/128$. The variant was situated in a conserved domain among several species (Fig. 2). Five tools were used to investigate the *in silico* predicted pathogenicity of the detected variant in *DCTN2* (Table 3). Of these, three predicted a neutral effect, while two predicted a disease causing or possible damaging effect. Similar findings were seen for the dynamitin mutagenesis protein variants that were used to investigate the protein–protein interactions important for dynactin structure (Table 3) (25).

The identified *GARS* variant, c.95T>C, did not segregate with the phenotype. The *GARS* variant, c.95T>C, was neither seen in in-house controls nor in dbSNP and ExAC databases. The variant was weakly conserved among species, and it was predicted benign in all variant prediction tools.

Exome sequencing revealed three other heterozygous variants on chromosome 12 in all five affected members probably sharing an ancestral haplotype.

The *DNAH10* gene is the force-generating protein of respiratory cilia and is a paralog to *DYNC1H1*, another CMT gene (ExAC and GeneCards (http://www.genecards.org/) databases).

DNAH10 is also expressed in brain, and it is not clear whether the ortholog in rat (Dlp10) is only involved in cilia function (26, 27). In addition, *DNAH10* might be expressed in peripheral nerves (http://www.proteinatlas.org/ENSG00000197653-DNAH10/tissue/soft + tissue).

Four tools were used to investigate the *in silico* predicted pathogenicity of the detected variant in *DNAH10*. Of these, one predicted a neutral effect, while three predicted a disease causing or probably damaging effect.

The *LRIG3* gene may play a role in craniofacial and inner ear morphogenesis during embryonic development (ExAC and GeneCards (http://www.genecards.org/) databases). Four tools were used to investigate the *in silico* predicted pathogenicity of the detected variant in *LRIG3*. Of these, three predicted a neutral effect, while one predicted a damaging effect.

The *MYO1A* gene is associated with non-syndromic hearing loss and deafness (ExAC and GeneCards (http://www.genecards.org/) databases). Four tools were used to investigate the *in silico* predicted pathogenicity of the detected variant in *MYO1A*. Of these, all predicted a neutral effect and the inferred change was in the last amino acid before stop.

Variant interpretation considerations

These variant prediction tools tend to disagree and are generally cautious in labeling a variant as having physical impact on the function of the gene (Table 3) (28). This further underlines the fact that there is to date no perfect *in silico* tools for mutation effect prediction and that genotype–phenotype correlation and functional assays are still the most important way to evaluate novel variants. The *DCTN2* gene is moderately conserved on the amino acid level (data not shown), and Fig. 2 shows the protein and the conservation on the exon 7 surrounding the c.337C>T variant are high for all mammals in the multiple sequence alignment. In addition, there is little normal variation in the gene (dbSNP and 1000 genomes). Our CMT family and C. elegans do share the Tyr residue at position 113 in *DCTN2*. The three other genes identified with heterozygous variants on chromosome 12 seem to have functions related to other organ systems.

Dynein–dynactin complex

DCTN2 overexpression in transgenic mice disrupts the dynein (DYNC1H1)–dynactin 0 (DCTN1) complex (7). *DYNC1H1* variants cause CMT2 and spinal muscular atrophy, while *DCTN1* variants cause distal hereditary motor neuronopathy (dHMN) (29–32). Thus, heterozygous variants in both *DYNC1H1* and *DCTN1* cause inherited neuropathies and neuronopathies. Neurophysiology in our family with the *DCTN2* variant is compatible with intermediate CMT (8).

DCTN2 encodes the protein dynamitin (p50), which is an element of dynactin, a highly conserved multiprotein complex (25, 33). Dynactin works in conjugation with the molecular motor dynein (encoded by *DYNC1H1*) and is responsible for retrograde transport in neurons, moving cargoes such as mitochondria, organelles, and proteins along the microtubules (34–37). Dynactin also has other functions independent of dynein such as attachment of microtubules to several subcellular structures (25, 33). Dynamitin is the core element of dynactin, four dynamitin subunits sit at the junction between dynactins two functional domains, the Arp1 filament binding cargo and the $p150^{Glued}$ (encoded by *DCTN1*), interacting with dynein and microtubules (25, 33). The expression of the dynactin molecule is highly regulated where dynamitin plays a key role probably due to its strong propensity for self-association. The overexpression of dynamitin monomers leads to disassembly of the dynactin-bound dynamitin, and association with the free monomers, this releases the $p150^{Glued}$ side chain which renders the remaining dynactin molecule non-functional (25, 33). Also, the depletion of dynamitin leaves the other subunits of dynactin unstable, leading to downregulation of the complex (33). The overexpression of *DCTN2* in transgenic mice results in a late-onset slowly progressive motor neuron degenerative disease (7).

The dynamitin molecule consists of three coiled-coil motifs, of which the two-first are predicted to mediate in self-association and stabilization of the whole dynactin complex. Sequence analysis predicts that particularity the first coiled-coil motif is especially important as this is the most conserved among species (Fig. 2) (25, 33).

The variant at position 113 (isoform 2) found in this family is situated in the first coiled-coil motif (Fig. 2).

The *DYNC1H1 paralog DNAH10* is expressed in the nervous system and may influence the dynein–dynactin complex or similar multiprotein complexes.

Conclusions

This is the first time a variant in the genes *DCTN2*, *DNAH10*, *LRIG3,* and *MYO1A* has been linked to an inherited neuropathy in humans.

However, our CMT family and C. elegans do share the Tyr residue at position 113 in *DCTN2*

and *DNAH10* may play a role in the nervous system. Hence, functional studies will be needed to confirm that these variants could be deleterious in humans. At the moment, no conclusion can be drawn concerning the causal role of the identified variants in the family phenotype. The haplotype with singular variants in *DCTN2*, *DNAH10*, *LRIG3,* and *MYO1A* is merely associated with CMT.

Acknowledgement

Øystein L. Holla and Linda Strand contributed in NGS, Hilde H. Hilmarsen contributed in Sanger sequencing and analysis, and Marit V. Svendsen designed the database. The study was financially supported by South-Eastern Norway Regional Health Authority, Akershus University Hospital HF, Telemark Hospital HF, and Nansen Foundation.

Conflicts of interest

The authors declare that they have no conflict of interests.

Authors' contribution

GJB acquired the material, conceived the study, participated in the design of the study, and drafted the manuscript. HH conceived the study, participated in the design of the study, and carried out the molecular genetic studies, sequence alignment, and bioinformatic analyses. ØLB and KT carried out the molecular genetic studies and bioinformatic analyses. CFS participated in the design of the study. MBR participated in the design of the study and drafted the manuscript. All authors critically read and approved the final manuscript.

References

1. Braathen GJ, Sand JC, Lobato A, Hoyer H, Russell MB. Genetic epidemiology of Charcot-Marie-Tooth in the general population. Eur J Neurol 2011;**18**:39–48.
2. Skre H. Genetic and clinical aspects of Charcot-Marie-Tooth's disease. Clin Genet 1974;**6**:98–118.
3. Combarros O, Calleja J, Polo JM, Berciano J. Prevalence of hereditary motor and sensory neuropathy in Cantabria. Acta Neurol Scand 1987;**75**:9–12.
4. Foley C, Schofield I, Eglon G, Bailey G, Chinnery PF, Horvath R. Charcot-Marie-Tooth disease in Northern England. J Neurol Neurosurg Psychiatry 2012;**83**:572–3.
5. Saporta AS, Sottile SL, Miller LJ, Feely SM, Siskind CE, Shy ME. Charcot-Marie-Tooth disease subtypes and genetic testing strategies. Ann Neurol 2011;**69**:22–33.
6. Murphy SM, Laura M, Fawcett K et al. Charcot-Marie-Tooth disease: frequency of genetic subtypes and guidelines for genetic testing. J Neurol Neurosurg Psychiatry 2012;**83**:706–10.
7. LaMonte BH, Wallace KE, Holloway BA et al. Disruption of dynein/dynactin inhibits axonal transport in motor neurons causing late-onset progressive degeneration. Neuron 2002;**34**:715–27.
8. Braathen GJ. Genetic epidemiology of Charcot-Marie-Tooth disease. Acta Neurol Scand Suppl 2012;**193**:iv-22.
9. Collins JS, Schwartz CE. Detecting polymorphisms and mutations in candidate genes. Am J Hum Genet 2002;**71**:1251–2.
10. Dyck PJ, Turner DW, Davies JL, O'Brien PC, Dyck PJ, Rask CA. Electronic case-report forms of symptoms and impairments of peripheral neuropathy. Can J Neurol Sci 2002;**29**:258–66.
11. Høyer H, Braathen GJ, Busk ØL et al. Genetic diagnosis of Charcot-Marie-Tooth disease in a population by next-generation sequencing. BioMed Research International 2014;**2014**:210401.
12. Holla OL, Bock G, Busk OL, Isfoss BL. Familial visceral myopathy diagnosed by exome sequencing of a patient with chronic intestinal pseudo-obstruction. Endoscopy 2014;**46**:533–7.
13. Li H, Durbin R. Fast and accurate short read alignment with Burrows-Wheeler transform. Bioinformatics 2009;**25**:1754–60.
14. DePristo MA, Banks E, Poplin R et al. A framework for variation discovery and genotyping using next-generation DNA sequencing data. Nat Genet 2011;**43**:491–8.
15. McKenna A, Hanna M, Banks E et al. The Genome Analysis Toolkit: a MapReduce framework for analyzing next-generation DNA sequencing data. Genome Res 2010;**20**:1297–303.
16. Wang K, Li M, Hakonarson H. ANNOVAR: functional annotation of genetic variants from high-throughput sequencing data. Nucleic Acids Res 2010;**38**:e164.
17. Adzhubei IA, Schmidt S, Peshkin L et al. A method and server for predicting damaging missense mutations. Nat Methods 2010;**7**:248–9.
18. Hicks S, Wheeler DA, Plon SE, Kimmel M. Prediction of missense mutation functionality depends on both the algorithm and sequence alignment employed. Hum Mutat 2011;**32**:661–8.
19. Ng PC, Henikoff S. Predicting deleterious amino acid substitutions. Genome Res 2001;**11**:863–74.
20. Schwarz JM, Rodelsperger C, Schuelke M, Seelow D. MutationTaster evaluates disease-causing potential of sequence alterations. Nat Methods 2010;**7**:575–6.
21. Johnson AD, Handsaker RE, Pulit SL, Nizzari MM, O'Donnell CJ, de Bakker PI. SNAP: a web-based tool for identification and annotation of proxy SNPs using HapMap. Bioinformatics 2008;**24**:2938–9.
22. Pollard KS, Hubisz MJ, Rosenbloom KR, Siepel A. Detection of nonneutral substitution rates on mammalian phylogenies. Genome Res 2010;**20**:110–21.
23. Siepel A, Bejerano G, Pedersen JS et al. Evolutionarily conserved elements in vertebrate, insect, worm, and yeast genomes. Genome Res 2005;**15**:1034–50.
24. Grantham R. Amino acid difference formula to help explain protein evolution. Science 1974;**185**:862–4.
25. Maier KC, Godfrey JE, Echeverri CJ, Cheong FK, Schroer TA. Dynamitin mutagenesis reveals protein-protein interactions important for dynactin structure. Traffic 2008;**9**:481–91.
26. Maiti AK, Mattéi MG, Jorissen M, Volz A, Zeigler A, Bouvagnet P. Identification, tissue specific expression, and chromosomal localisation of several human dynein heavy chain genes. Eur J Hum Genet 2000;**8**:923–32.
27. Tanaka Y, Zhang Z, Hirokawa N. Identification and molecular evolution of new dynein-like protein sequences in rat brain. J Cell Sci 1995;**108**(Pt 5):1883–93.
28. Castellana S, Mazza T. Congruency in the prediction of pathogenic missense mutations: state-of-the-art web-based tools. Briefings in Bioinformatics 2013;**14**:448–59.

29. Weedon MN, Hastings R, Caswell R et al. Exome sequencing identifies a DYNC1H1 mutation in a large pedigree with dominant axonal Charcot-Marie-Tooth disease. Am J Hum Genet 2011;**89**:308–12.
30. Harms MB, Ori-McKenney KM, Scoto M et al. Mutations in the tail domain of DYNC1H1 cause dominant spinal muscular atrophy. Neurology 2012;**78**:1714–20.
31. Puls I, Jonnakuty C, LaMonte BH et al. Mutant dynactin in motor neuron disease. Nat Genet 2003;**33**:455–6.
32. Munch C, Sedlmeier R, Meyer T et al. Point mutations of the p150 subunit of dynactin (DCTN1) gene in ALS. Neurology 2004;**63**:724–6.
33. Jacquot G, Maidou-Peindara P, Benichou S. Molecular and functional basis for the scaffolding role of the p50/dynamitin subunit of the microtubule-associated dynactin complex. J Biol Chem 2010;**285**:23019–31.
34. Schnapp BJ, Reese TS. Dynein is the motor for retrograde axonal transport of organelles. Proceedings of the National Academy of Sciences of the USA 1989;**86**:1548–52.
35. Eschbach J, Dupuis L. Cytoplasmic dynein in neurodegeneration. Pharmacol Ther 2011;**130**:348–63.
36. Hafezparast M, Klocke R, Ruhrberg C et al. Mutations in dynein link motor neuron degeneration to defects in retrograde transport. Science 2003;**300**:808–12.
37. Schroer TA, Steuer ER, Sheetz MP. Cytoplasmic dynein is a minus end-directed motor for membranous organelles. Cell 1989;**56**:937–46.